Calculation of Two-Dimensional Turbulent Boundary Layers over Rigid and Moving Wavy Surfaces

T. K. Sengupta* and S. G. Lekoudis†
Georgia Institute of Technology, Atlanta, Georgia

A technique is presented for computing turbulent boundary layers over rigid and moving sinusoidal wavy surfaces. The technique consists of an iterative coupling between solutions of the boundary layer, and solutions of an Orr-Sommerfeld-type system. The predicted pressure distributions and total drag agree well with recent measurements for rigid wavy surfaces. For moving surfaces the calculation is a prediction of steady streaming. Comparisons are made with measurements of airflow over deep water waves.

I. Introduction

THE problem of reducing drag due to skin friction remains of interest due to the significant benefits that would result from an application of a drag-reducing scheme on airplanes, ships, or underwater vehicles. One of the techniques proposed for drag reduction is the use of compliant walls. It has been proposed that compliant walls may delay transition, or may modify a turbulent boundary layer with the result of smaller skin friction values. A summary of recent efforts directed toward inventing a working system is given in Ref. 1.

In this paper, calculations of turbulent boundary layers over stationary and moving wavy surfaces are presented. The flow is assumed to be two-dimensional and incompressible. The fluid/compliant coating interaction problem is not solved. The authors are not interested in the material characteristics of the wall that generate a particular flow. Rather, they look for a specified wall motion that generates a flow with low skin friction. With this objective in mind the problem becomes that of finding a particular wall motion that produces a flow with low skin friction. In the modeling of the flow an assumption is made: The coherent events that occur in the turbulent boundary layer are not explicitly modeled. The time-averaged equations are used. The reasonably good comparison between calculations and measurements indicates that the time-averaged equations do not lead to unrealistic results.

Incompressible, two-dimensional, boundary-layer flow over wavy surfaces has been examined in Refs. 2-13. Both analytical and experimental work is reported. The analytical approaches can be categorized into three groups. The first group involves perturbation techniques.[6-8] The second group deals with boundary layers with curvature.[9] The third group solves the time-averaged Navier-Stokes equations.[10-13] Most of the experiments were done for flows over stationary wavy surfaces. The available measurements for the case of moving walls are scarce, with the exception of Ref. 3.

In this paper a technique is presented for computing turbulent boundary-layer flows over stationary and moving wavy surfaces. The technique consists of an iterative coupling between solutions of the boundary-layer equations and those of an Orr-Sommerfeld system. The Orr-Sommerfeld system computes the disturbance flow generated from the presence of the wavy boundary. The analytical formulation is given in Sec. II. The numerical formulation is given in Sec. III. The computations for stationary walls are given in Sec. IV, and for moving walls in Sec. V. Finally, the concluding remarks are given in Sec. VI.

II. Analytical Formulation

The two-dimensional flow of an incompressible fluid with constant properties is prescribed in an x, y, z Cartesian system by the Navier-Stokes equations in conservation form[14]:

$$\frac{\partial \bar{W}}{\partial t}+\frac{\partial \bar{F}}{\partial x}+\frac{\partial \bar{G}}{\partial y}=\frac{\partial \bar{F}_1}{\partial x}+\frac{\partial \bar{G}_1}{\partial y} \tag{1a}$$

$$\bar{W}=\begin{vmatrix} 1 \\ u \\ v \end{vmatrix}, \quad \bar{F}=\begin{vmatrix} u \\ u^2+p/\rho \\ uv \end{vmatrix}, \quad \bar{G}=\begin{vmatrix} v \\ uv \\ v^2+p/\rho \end{vmatrix} \tag{1b}$$

$$\bar{F}_1=\begin{vmatrix} 0 \\ \frac{2}{3}\nu\left(2\frac{\partial u}{\partial x}-\frac{\partial v}{\partial y}\right) \\ \nu\left(\frac{\partial u}{\partial y}+\frac{\partial v}{\partial x}\right) \end{vmatrix}, \quad \bar{G}_1=\begin{vmatrix} 0 \\ \nu\left(\frac{\partial u}{\partial y}+\frac{\partial v}{\partial x}\right) \\ \frac{2}{3}\nu\left(2\frac{\partial v}{\partial y}-\frac{\partial u}{\partial x}\right) \end{vmatrix} \tag{1c}$$

In Eqs. (1), u and v denote the velocity components in the x and y directions, respectively, ν is the kinematic viscosity, and t the time. Using an arbitrary time-dependent transformation to an orthogonal coordinate system S, N, Eqs. (1) become:

$$\frac{1}{J}\frac{\partial \bar{W}}{\partial t}+\frac{\partial \bar{F}'}{\partial S}+\frac{\partial \bar{G}'}{\partial N}=\frac{\partial \bar{F}_1'}{\partial S}+\frac{\partial \bar{G}'}{\partial N} \tag{2a}$$

$$J=\frac{\partial (S,N)}{\partial (x,y)} \tag{2b}$$

$$\bar{F}'=\frac{\bar{F}}{J}\frac{\partial S}{\partial x}+\frac{\bar{G}}{J}\frac{\partial S}{\partial y} \tag{2c}$$

$$\bar{G}'=\frac{\bar{F}}{J}\frac{\partial N}{\partial x}+\frac{\bar{G}}{J}\frac{\partial N}{\partial y} \tag{2d}$$

$$\bar{F}_1'=\frac{\bar{F}_1}{J}\frac{\partial S}{\partial x}+\frac{\bar{G}_1}{J}\frac{\partial S}{\partial y} \tag{2e}$$

$$\bar{G}_1'=\frac{\bar{F}_1}{J}\frac{\partial N}{\partial x}+\frac{\bar{G}_1}{J}\frac{\partial N}{\partial y} \tag{2f}$$

A coordinate system[6] is introduced wherein the wavy surface is a coordinate line which degenerates into a Cartesian system

Presented as Paper 83-1670 at the AIAA 16th Fluids and Plasma Dynamics Conference, Danvers, Mass., July 12-14, 1983; received July 21, 1983; revision received May 30, 1984. Copyright © American Institute of Aeronautics and Astronautics, Inc., 1983. All rights reserved.

*Graduate Research Assistant, School of Aerospace Engineering. Student Member AIAA.

†Associate Professor, School of Aerospace Engineering. Member AIAA.

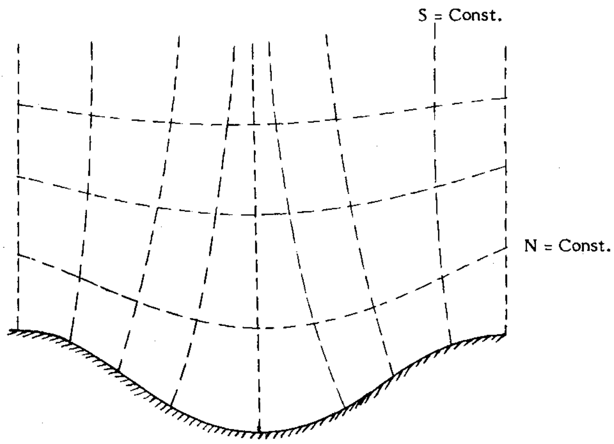

Fig. 1 Coordinate system.

far from the wavy surface. The coordinate system moves with the phase speed, the complex notation is introduced for convenience, and the coordinate system is shown in Fig. 1.

$$S=(x-ct)-i\epsilon e^{-ky}e^{ik(x-ct)} \tag{3a}$$

$$N=y-\epsilon e^{-ky}e^{ik(x-ct)} \tag{3b}$$

where ϵ is the wave amplitude, k the wavenumber, and c the phase velocity. In this paper the normalizing parameters are the local displacement thickness and freestream velocity of the boundary layer. The velocity components in the S, N coordinate system can be obtained using chain rule with the following results:

$$v_s=\frac{\partial S}{\partial t}+u\frac{\partial S}{\partial x}+v\frac{\partial S}{\partial y} \tag{4a}$$

$$v_N=\frac{\partial N}{\partial t}+u\frac{\partial N}{\partial x}+v\frac{\partial N}{\partial y} \tag{4b}$$

All of the flow quantities are decomposed into a mean, time-independent part, a fluctuating part due to turbulence, and a periodic part attributed to the presence of the wavy surface.[15] In the equations that follow, C.C. denotes complex conjugate.

$$v_s(s,N,z,t)=\bar{U}(S,N)+u'(x,N,z,t)+\epsilon[\tilde{u}(N)e^{ikS}+\text{C.C}] \tag{5a}$$

$$v_N(s,N,z,t)=\bar{V}(S,N)+v'(S,N,z,t)+\epsilon[\tilde{v}(N)e^{ikS}+\text{C.C.}] \tag{5b}$$

$$p(S,N,z,t)=\bar{P}(S,N)+p'(S,N,z,t)+\epsilon[\tilde{p}(N)e^{ikS}+\text{C.C.}] \tag{5c}$$

The following assumptions will be made with the use of Eqs. (5). The mean flow, assumed locally parallel, is obtained from the boundary-layer equations. The flow component due to the presence of the wavy boundary is proportional in magnitude to the wave amplitude and periodic in space and time. If one rearranges Eqs. (4), the velocities in the x, y Cartesian system are obtained as functions of the velocities in the S, N curvilinear system:

$$u=J^{-1}\left(v_s\frac{\partial N}{\partial y}-v_N\frac{\partial S}{\partial y}+\frac{\partial N}{\partial t}\frac{\partial S}{\partial y}-\frac{\partial S}{\partial t}\frac{\partial N}{\partial y}\right) \tag{6a}$$

$$v=J^{-1}\left(v_N\frac{\partial S}{\partial x}-v_S\frac{\partial N}{\partial x}+\frac{\partial S}{\partial t}\frac{\partial N}{\partial x}-\frac{\partial N}{\partial t}\frac{\partial S}{\partial x}\right) \tag{6b}$$

Then, the combination of Eqs. (5) and (6) gives the velocities in the Cartesian system as follows:

$$u=\bar{U}+c+u'+e^{ikS}\epsilon[\tilde{u}-ke^{-kN}(\bar{U}+u'+iv')] \tag{7a}$$

$$v=\bar{v}+v'+e^{ikS}\epsilon[\tilde{v}-ke^{-kN}(\tilde{v}'-i\bar{U}-iu')] \tag{7b}$$

A. Mean Flow

The mean flow is obtained by "bending" a boundary-layer flow to follow the wavy surface. The governing equations are obtained as follows. The triple decomposition, expressed in Eqs. (5), is substituted into Eqs. (2). The resulting equation is time averaged. The boundary-layer assumptions are implemented and the terms due to curvature are neglected. The resulting equations are as follows:

$$\frac{\partial \bar{U}}{\partial S}+\frac{\partial \bar{V}}{\partial N}=0 \tag{8a}$$

$$\bar{U}\frac{\partial \bar{U}}{\partial S}+\bar{V}\frac{\partial \bar{U}}{\partial N}=-\frac{1}{\rho}\frac{\partial \bar{P}}{\partial S}+\frac{\partial}{\partial N}\left(\nu\frac{\partial \bar{U}}{\partial N}-\overline{u'v'}-\text{WS}\right) \tag{8b}$$

$$\text{WS}=(\epsilon^2/4)(\tilde{u}^*\tilde{v}+\tilde{u}\tilde{v}^*) \tag{8c}$$

Some discussion is necessary regarding the approximations that give Eq. (8b). Obviously the WS terms are of $\mathcal{O}(\epsilon^2)$ and are a result of the time-averaged nonlinear products of harmonic in time terms. Only the first harmonic is retained. The $\partial/\partial S$ of other $\mathcal{O}(\epsilon^2)$ terms in Eq. (8b) have been neglected, not because of the boundary-layer/parallel-flow assumption for the mean flow, but because of their functional independence on S. Careful observation shows that these terms, like the WS terms in Eq. (8c), are independent of S due to time averaging. This is the case in spite of the fact that they may be much larger than the remaining WS terms. It is their S derivative that, being identically zero, is not contributing in the Eq. (8b). The *DC* terms that contribute in the N-momentum equation would affect the mean pressure inside the boundary layer to $\mathcal{O}(\epsilon^2)$. Therefore, they are neglected because the wave effects on the pressure are computed to $\mathcal{O}(\epsilon)$ and, therefore, are much larger than the neglected terms. The Reynolds stresses due to the fluctuating turbulent velocities are modeled using the Cebeci-Smith eddy-viscosity model.[16] However, because of the presence of the wavy wall, these stresses do not remain the same. Therefore, from experimental observations, it is assumed that the Reynolds stresses deviate sinusoidally from their mean values as follows[17,18]:

$$\overline{u'v'}=(\overline{u'v'})_m[1-r(N)e^{ikS}] \tag{9}$$

The evaluation of $r(N)$ becomes a problem in turbulence modeling. Several models were tested,[8] and one based on lag coefficients for the pressure in the law of the wall was found to be superior.[8] Navier-Stokes calculations were performed with[13] and without[12] the modification of the eddy-viscosity described in Eq. (9). Both showed good agreement with experiments. In Ref. 13 it is reported that using the model was necessary in order to obtain good comparison with experiments for the phase of the wall shear stress. In the present study the same was found. The modeling of $r(N)$ in the present work agrees with the findings of Ref. 8. The boundary conditions for the mean flow are that $\bar{V}=0$ on $N=0$ and far from the wall, $\bar{U}$ approaches freestream values that are given functions of S. The value of $\bar{U}$ at the wall depends on the wall motion.

B. Disturbance Flow

The disturbance flow is obtained using the following procedure. The triple decomposition expressed with Eqs. (5) is substituted into Eqs. (2); the mean flow is assumed to be locally parallel; a phase averaging of the equations is performed; a time averaging of the equations is performed; the latter is subtracted from the former; finally the effect of the WS on the resulting equation is neglected (linearization of the disturbance flow). The resulting system of equations is a nonhomogeneous Orr-Sommerfeld system that can be expressed in the following form:

$$\frac{\mathrm{d}z_i}{\mathrm{d}N} = \sum_{j=1}^{4} a_{ij} z_j + b_i \tag{10}$$

where $z_1 = \tilde{u}$, $z_2 = \mathrm{d}\tilde{u}/\mathrm{d}N$, $z_3 = \tilde{v}$, $z_4 = \tilde{p}$, and the coefficients a_{ij} and b_i are defined in the Appendix.

The boundary conditions for Eq. (10) are as follows. Far from the wall the coordinate system approaches a Cartesian system and the solution of Eq. (10) approaches the analytical solution of the classical Orr-Sommerfeld system. Therefore, it is imposed that the exponentially growing modes are suppressed, which provides two boundary conditions. The other two boundary conditions are provided from conditions at the wall.

At the wavy surface $N=0$, the fluctuating velocity due to turbulence vanishes and Eqs. (7) can be rewritten as follows:

$$\epsilon \tilde{u} = \frac{u - \bar{U} - c}{e^{ikS}} + k\bar{U} \tag{11a}$$

$$\epsilon \tilde{v} = \frac{v}{e^{ikS}} - ik\bar{U} \tag{11b}$$

Therefore, if the wall motion is specified in the original x, y Cartesian system by specifying the velocity components u and v, and the mean flow $\bar{U}$ is determined, Eqs. (11) provide the two boundary conditions needed to solve the system of Eq. (10).

III. The Numerical Procedure

The mean flow is obtained from a finite difference solution of the turbulent boundary-layer equations for two-dimensional incompressible flow with arbitrary pressure gradients. The solution procedure uses the Keller box and the algebraic eddy-viscosity model of Cebeci and Smith.[16] The system of Eq. (10) has the classical numerical difficulties of an Orr-Sommerfeld system; therefore, an orthonormalization procedure was used.[19]

The iterative coupling between the Orr-Sommerfeld system and the solution of the boundary-layer equations is due to the existence of the wave-induced stresses, described by Eq. (8c). No more than three iterations are needed to obtain a converged solution. Convergence was checked by requiring that the percentage change of the slope of the mean velocity profile was less than one-thousandth at the final iteration. This is a much more strict convergence than the one usually used for the boundary-layer equations; however, it was found to be necessary because the disturbance flow varies very rapidly close to the wall.

IV. Results and Discussion

A. Flows Over Rigid Wavy Surfaces

The linear solution for laminar flow was tested by comparing with Benjamin's[6] results. However, some comments are appropriate regarding Benjamin's theory.[6] He used a surface-conforming coordinate system. In the final solution he neglected the nonhomogeneous (b_i) terms that the coordinate system brings into the differential equations. This makes the answer equivalent to the one obtained in a Cartesian system for other than simple linear laminar mean profiles. Because the Cartesian system places severe restrictions on the wave amplitude, it is incorrect to blame the linearization procedure for poor results as the wave amplitude increases. These poor results are due to the neglect of the nonhomogeneous terms.

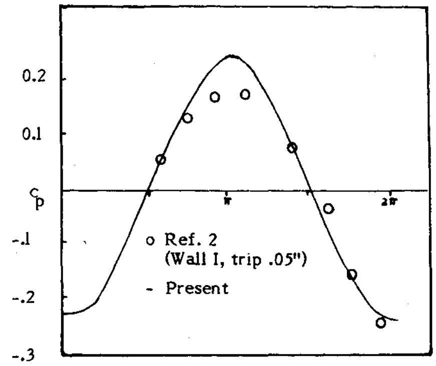

Fig. 2 Calculated and measured C_p for Sigal's experiment.[2]

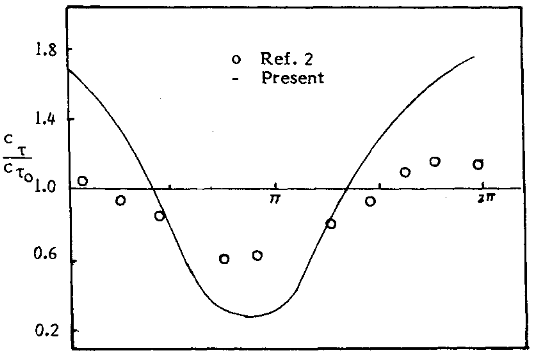

Fig. 3 Calculated and measured skin friction for Sigal's experiment.[2]

Also, all of the previous investigators that used a perturbation approach neglected the "viscous" solution at some distance away from the wall. The case computed by Thorsness et al.[8] is analyzed next. Although this is a calculation for laminar flow, the wall friction velocity is used to normalize the mean flow given by $\bar{u} = (2\delta/\pi)\sin(\pi y/2)$ for $0 \leq y < \delta$ and $\bar{u} = 2\delta/\pi$ for $y > \delta$. The streamwise Reynolds number Rx is 800,000 and $x/\lambda = 5.94$, where λ is the wavelength. Also δ is equal to 2.75 $Rx^{0.25}$. Benjamin's results for the nondimensional pressure and its phase are 4.67×10^{-4} and 181.86 deg, respectively. The authors found 4.48×10^{4} and 182.05 deg. However, while the amplitude and phase of the shear perturbation are 0.083076 and 45.2 deg, respectively,[6] the authors computed 0.055 and 44.5 deg. When the authors computed in the Cartesian system they found 0.093 and 45.1 deg for the shear and its phase. The small difference between this last result and what Benjamin's[6] theory gives is due to his neglect of the viscous mode in the freestream. From the above it is evident that the coordinate system can have a large effect in the answer, especially for the shear.

Because the disturbance flow is obtained from a linearization procedure, it is useful to check the validity of the developed formulation as the wave amplitude increases for turbulent flow. For the cases considered, the linear momentum equations predicted separation for amplitude to wavelength ratios higher than approximately 0.022. Because the flow does approach separation at these amplitudes and the higher harmonics become important, the formulation should not be applied to waves with these characteristics. Because we are dealing with turbulent flow the validity of the theoretical assumptions cannot be rationalized in any other way but by comparing with measurements. The data of Kendall[3] are for an amplitude to wavelength ratio of 0.031 and the present theory cannot handle such large amplitude waves.

A comparison with the measurements of Ref. 2 is shown in Figs. 2 and 3. The agreement is reasonable only for the pressure. However, these data are for amplitude to wavelength ratios of 0.028 and the effect of linearization is evident in the inaccurate prediction of the shear.

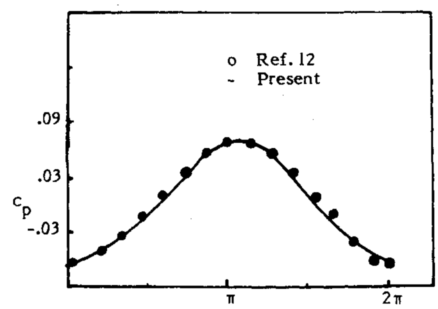

Fig. 4 Calculated and measured pressure coefficient for NASA Langley's experiment.

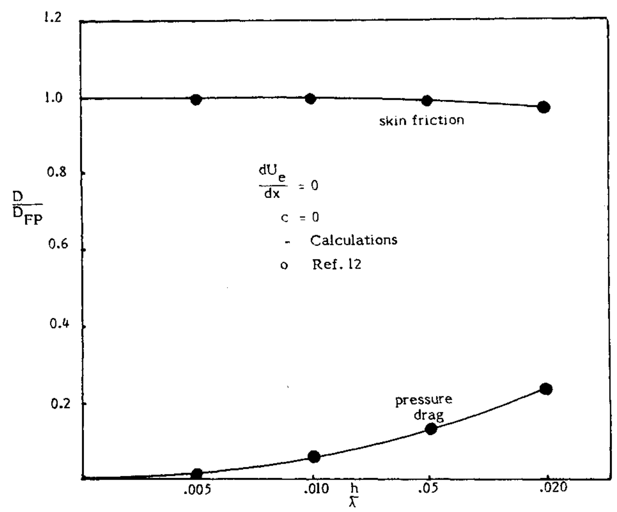

Fig. 5 Calculated and measured drag components.

Several geometries were examined at NASA Langley.[12] Figure 4 shows predicted and measured pressure coefficients. The measured data were reproduced from Fig. 7 of Ref. 12. The agreement is good. Figure 5 shows predicted and measured drag coefficients. The measured data were reproduced from Fig. 5 of Ref. 12. The level of agreement is of the same quality as that obtained from Navier-Stokes solvers.[12] This lends credibility to the assumptions used in the developed formulation. Moreover it makes the predictions for the case of moving walls, where experiments are scarce, more credible. The developed procedure does reproduce the observed reduction in the mean skin friction, something impossible to obtain with a linear theory. Some discussion is warranted on the role of skin friction, based on observations made during the present study.

It can easily be shown that the contribution of the spatially oscillating skin friction to drag is zero to $\mathcal{O}(\epsilon^2)$. However, to the same of $\mathcal{O}(\epsilon^2)$, the oscillating pressure creates the pressure drag. Therefore, for these flows, it is much more important to predict the mean skin friction and oscillatory pressure accurately. From another point of view, mispredicting the phase and amplitude of the oscillatory shear does not show in comparisons of total drag levels. Examining experiments from this point of view makes the model of the oscillating Reynolds stresses less important, unless this modeling affects, even in small ways, the oscillating pressure.

The authors also investigated turbulent flow over a rigid wavy wall with pressure gradients. The geometry is identical to the one used at NASA Langley.[12] The pressure gradient was created by changing the local freestream velocity linearly between $x = 5.75$ ft and the end of the plate. The velocity at the end of the plate was 91.312 ft/s for the case of the favorable pressure gradient and 72.756 ft/s for the case of the adverse pressure gradient. No significant effects of the pressure gradient were found, and there are no experiments to substantiate this conclusion.

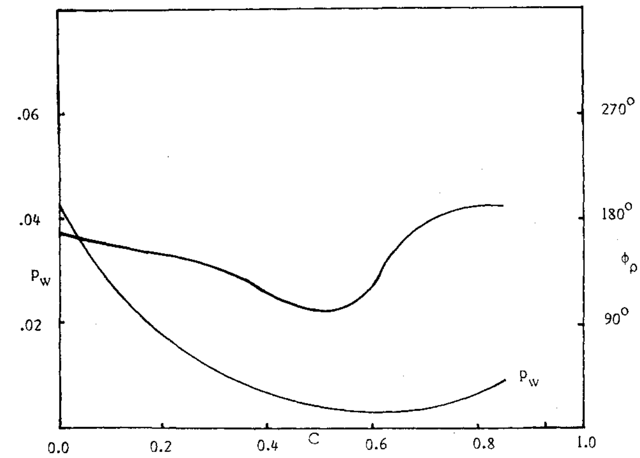

Fig. 6 Variation of the amplitude and phase of the pressure with phase speed.

B. Flows Over Moving Wavy Surfaces

The authors also investigated flows over moving surfaces. For the case of a wave with phase speed c, the mean flow has a velocity $\bar{U} - c$ with respect to the moving frame, and the mean velocity at the wall is equal to $-c$. From the equation of the body surface for a cosine wave

$$y_b = \epsilon e^{ik(x-ct)} \tag{12}$$

the linearized velocity component in the y direction is obtained

$$v = -ikcy_b \tag{13a}$$

The u component of the velocity depends on the particular surface motion. For example, for a rigid wave translating with velocity c, the inviscid perturbation velocity of the flow above it is given by

$$u = -kcy_b \tag{13b}$$

Equation (13b) can be obtained from the solution of the potential flow over a rigid translating cosine wave. If the wavy surface is due to the motion of a deep water cosine wave, then the u-velocity component is given by

$$u = kcy_b \tag{13c}$$

These boundary conditions can be used with Eqs. (11) to give

$$\tilde{v} = 0 \tag{14a}$$

$$\tilde{u} = -2kc \tag{14b}$$

or

$$\tilde{u} = 0 \tag{14c}$$

Both boundary conditions (14b) and (14c) were used. The only difference in the result is the variation of the phase of the oscillating shear with the wave speed. All of the other quantities showed small quantitative, never qualitative, differences. This suggests that all of the other surface motions inside the range of the conditions described by Eqs. (14) most probably behave the same way. Cases where the surface executed water wave motion of finite depth were also examined. In this case the surface particles execute elliptical orbital motions which become circular for deep water waves. Again, with the exception of the phase of the shear, no significant quantitative, and never qualitative, differences were obtained between the elliptical and circular motions. Considering the negligible effect of the phase of the oscillating shear on the drag, the results shown next are representative of all of the cases.

The variation of the amplitude and phase of the pressure are plotted in Fig. 6. Although the amplitude of the oscillating pressure decreases with phase speed, the variation of the phase

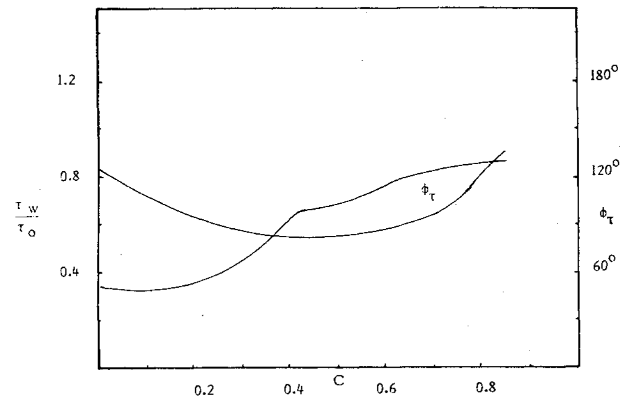

Fig. 7 Variation of the amplitude and phase of oscillatory shear with phase speed.

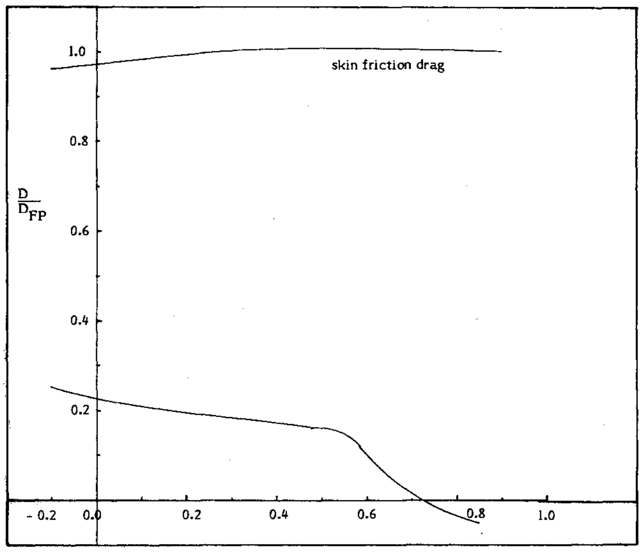

Fig. 8 Variation of the skin friction and pressure drag components with phase speed.

is drag producing. However, as the phase speeds approach the freestream speeds, the phase of the pressure produces thrust. The variation of the amplitude and phase of the oscillating shear is shown in Fig. 7. These results are for a surface motion simulating deep water wave and with the viscous boundary condition [Eq. (14c)]. The results shown in Figs. 6 and 7 are in qualitative agreement with Kendall's measured data.[3] However, because these data are for an amplitude to wavelength ratio of 0.03, the present formulation indicated separation and direct quantitative comparison is not possible.

The drag values normalized with those of the equivalent flat plate are plotted in Fig. 8. The plate geometry and flow conditions are identical with those of Langley's experimental setup[12] and the amplitude to wavelength ratio of the waves used is 0.02. The skin friction reduction diminishes at the higher wave speeds but the phase of the pressure indicates thrust. Because the turbulence model was developed for zero phase speeds, the high-speed results need experimental verification. This prompted the authors to examine some new experiments.[17,18]

The experiments reported in Refs. 17 and 18 deal with air turbulent boundary layers over deep water waves. Detailed measurements of the perturbation components of the velocity are given. Figures 9-12 show the variation of the amplitude and phase of the oscillatory velocity components. The agreement between the predictions and measurements is reasonable. In general, the comparison between calculations and experiments becomes worse at the higher phase speeds. The good agreement between the calculations and measured data for phase speeds up to about 0.7 times the freestream speed gives confidence in the drag predictions for this range of speeds. This is because the theory predicts not only surface quantities, but the variation of flow properties inside the turbulent boundary layer.

Some discussion is appropriate regarding the effect of the initial conditions on the results. Small changes in the initial conditions can have significant effects on the results, especially the shear. In all of the comparisons the initial conditions for the turbulent boundary layer were matched with the measured conditions upstream of the waves. Therefore the flow without the wave-induced disturbances was identical to the measured flow.

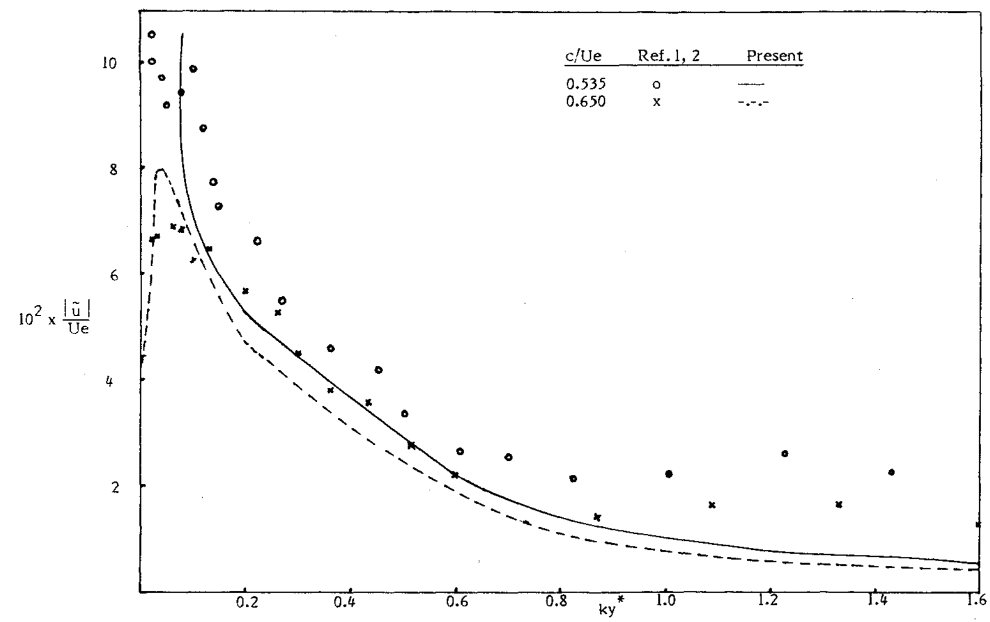

Fig. 9 Variation of the amplitude of the streamwise perturbation velocity component above the wave. Measurements from Refs. 17 and 18.

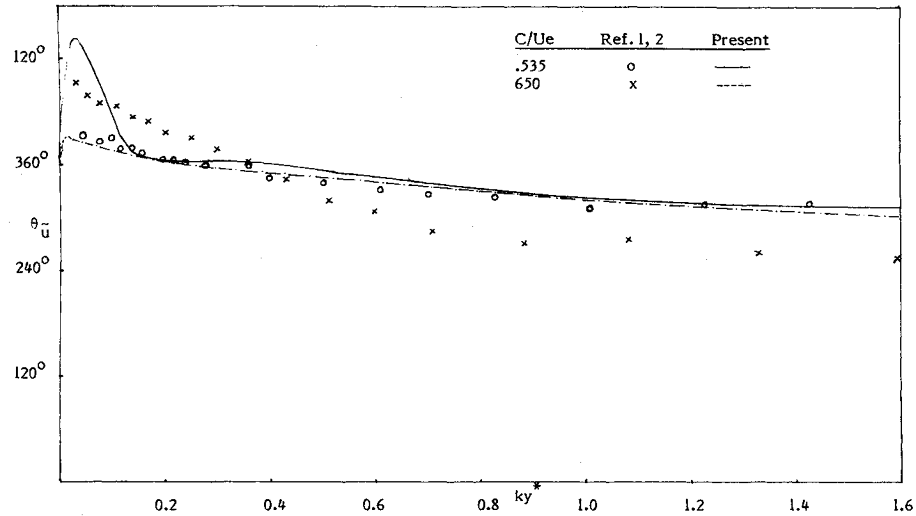

Fig. 10 Variation of the phase of streamwise perturbation velocity component above the wave. Measurements from Refs. 17 and 18.

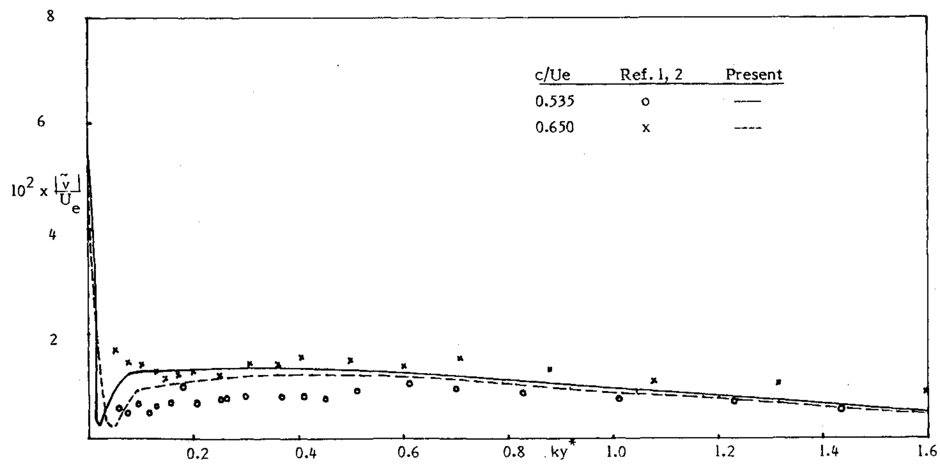

Fig. 11 Variation of the amplitude of normal perturbation velocity component above the wave. Measurements from Refs. 17 and 18.

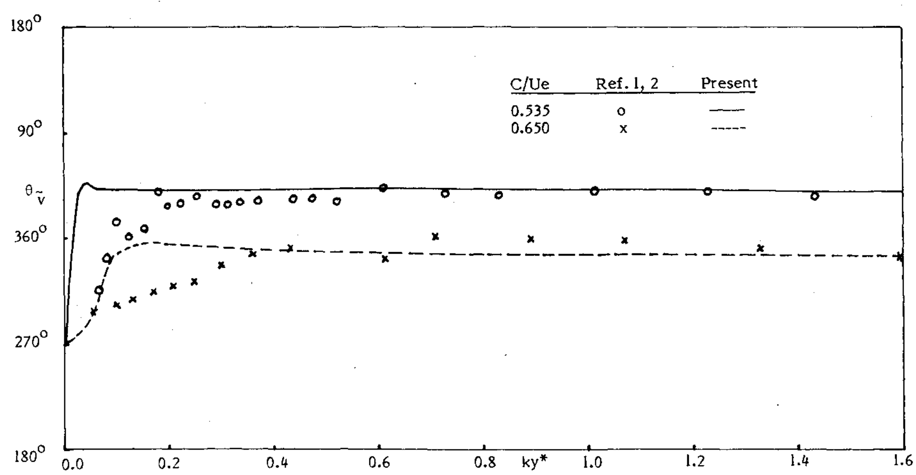

Fig. 12 Variation of the phase of normal perturbation velocity component above the wave. Measurements from Refs. 17 and 18.

V. Concluding Remarks

A numerical technique was developed for computing turbulent boundary layers over rigid or moving wavy surfaces. The technique was tested by comparison with experiments. The following remarks are appropriate:

1) The technique predicts the flows over rigid wavy surfaces correctly, at least for the case of lower amplitude waves, such as measured in Ref. 12.

2) For accurate estimations of the total drag, the most important quantities are the amplitude and phase of the pressure and the mean shear. The reason is that they are the main contributors to drag.

3) For the types of wall motion considered, the technique predicted no drag reduction, except for the case of wave speeds approaching the freestream speed. In all other cases the pressure drag overpowers the mean skin friction reduction generated by the waves.

4) Reasonable quantitative agreement was obtained with measurements *inside* the turbulent boundary layer over water waves for nondimensional phase speeds of up to 7/10.

Appendix

The coefficients a_{ij} and b_i of the Orr-Sommerfeld system [Eq. (10)] are

$$a_{11}=a_{13}=a_{14}=b_1=0 \tag{A1}$$

$$a_{12}=1 \tag{A2}$$

$$a_{21}=R\left[k_h^2+k^2RU_3\frac{(2+U_6)}{U_2}\right]\Big/U_8 \tag{A3}$$

$$a_{22}=\left[+\frac{U_4(2+U_6)}{U_2}-\frac{U_3U_5}{U_2^2}(2+U_6)+\frac{U_3U_7}{U_2}-U_3U_6P_2a_{24}\right]R/U_8 \tag{A4}$$

$$a_{23}=[U_2+ikU_4(2+U_6)/U_2-ikU_5U_3(2+U_6)/U_2^2-P_2U_3U_6a_{43}+ikU_3U_7/U_2]R/U_8 \tag{A5}$$

$$a_{24}=[ik-P_2U_4U_6-P_2U_3(U_7+U_6a_{44})]R/U_8 \tag{A6}$$

$$b_2=bR\Big\{-ik\bar{U}^2+4kU_3+m(\delta^*/x^*)+U_4(2U_6-2k\bar{U}(2+U_6)/U_2)+U_3\left[2k(2+U_6)\left(\frac{\bar{U}U_5}{U_2^2}-2\right)-P_2U_4U_6/b\right]+\frac{U_5}{R}-\frac{2k}{R}U_2+2U_3U_7\left(1-\frac{k\bar{U}}{U_2}\right)\Big\}\Big/U_8 \tag{A7}$$

$$a_{31}=-ik \tag{A8}$$

$$a_{32}=a_{33}=a_{34}=0 \tag{A9}$$

$$b_3=2ik^2e^{-kN}\bar{U} \tag{A10}$$

$$a_{41}=0 \tag{A11}$$

$$a_{42}=-\frac{ik}{R}-ikU_3\frac{(2+U_6)}{U_2} \tag{A12}$$

$$a_{43}=-\frac{k_h^2}{R}+k^2U_3\frac{(2+U_6)}{U_2} \tag{A13}$$

$$a_{44}=ikU_3U_6P_2 \tag{A14}$$

$$b_4=\left[k\bar{U}^2-\frac{2ik^2\bar{U}}{R}-iU_4+4ikU_3+\frac{iU_5}{R}-2ikU_3(2+U_6)\left(1-\frac{k\bar{U}}{U_2}\right)\right]b \tag{A15}$$

$$P_2=\frac{2ikk_1}{1+ikk_L} \tag{A16}$$

$$U_2=\frac{d\bar{U}}{dN} \tag{A17}$$

$$U_3=(\overline{u'v'})_m \tag{A18}$$

$$U_4=\frac{d}{dN}(\overline{u'v'})_m \tag{A19}$$

$$U_5=\frac{d^2\bar{U}}{dN^2} \tag{A20}$$

$$U_6=\bar{D}\exp(-\bar{D})/[1-\exp(-\bar{D})] \tag{A21}$$

$$\bar{D}=(Nu_T)/(A^+) \tag{A22}$$

$$U_7=\frac{dU_6}{dN} \tag{A23}$$

$$U_8=-\frac{1}{R}+\frac{U_3}{U_2}(2+U_6) \tag{A24}$$

$$k_h^2=k^2+ikR\bar{U} \tag{A25}$$

$$b=ke^{-kN} \tag{A26}$$

In the above equations, R is the Reynolds number, k_1 and k_L the modeling constants,[8] u_T the wall friction velocity, and A^+ the constant in the law of the wall.

Acknowledgments

This work was supported by the Compliant Coating Drag Reduction Program of the Office of Naval Research with the Contracts N00014-82-k-0271 and N00014-83-k-0418.

References

[1] Abstracts of the Drag Reduction Symposium held at the National Academy of Sciences in Washington, D.C., Sept. 1982.

[2] Sigal, A., "An Experimental Investigation of the Turbulent Boundary Layer Over a Wavy Wall," Ph.D. Thesis, California Institute of Technology, Pasadena, Calif., 1971.

[3] Kendall, J., "The Turbulent Boundary Layer Over a Wall with Progressive Surface Waves," *Journal of Fluid Mechanics*, Vol. 41, Pt. 2, 1970, pp. 259-281.

[4] Zilker, D. P., Cook, G. W., and Hanratty, T. J., "Influence of the Amplitude of a Solid Wavy Wall on a Turbulent Flow, Part 1, Non-Separated Flows," *Journal of Fluid Mechanics*, Vol. 82, Pt. 1, 1977, pp. 29-51.

[5] Silker, D. P. and Hanratty, T. J., "Influence of the Amplitude of a Solid Wavy Wall on a Turbulent Flow, Part 2, Separated Flows," *Journal of Fluid Mechanics*, Vol. 90, Pt. 2, 1979, pp. 257-271.

[6] Benjamin, T. B., "Shearing Flow Over a Wavy Boundary," *Journal of Fluid Mechanics*, Vol. 6, 1959, pp. 161-205.

[7] Lekoudis, S. G., Nayfeh, A. H., and Saric, W. S., "Compressible Boundary Layers Over Wavy Walls," *Physics of Fluids*, Vol. 19, No. 4, 1976, pp. 574-519.

[8] Thorsness, C. B., Morrisroe, P. E., and Hanratty, T. J., "A Comparison of Linear Theory with Measurements of the Variation of Shear Stress Along a Solid Wave," *Chemical Engineering Science*, Vol. 33, 1978, pp. 579-592.

[9] Cary, A. M., Weinstein, L. M., and Bushnell, D. M., "Drag Reduction Characteristics of Small Amplitude Rigid Surface Waves," *Viscous Flow Drag Reduction, Progress in Astronautics and Aeronautics*, Vol. 72, AIAA, New York, 1980, pp. 144-167.

[10] Balasubramanian, R. and Orszag, S. A., "Numerical Simulation of Flow Over Wavy Walls," AIAA Paper 80-1350, 1980.

[11] Caponi, E. A., Fornberg, B., Knight, D. D., McLean, J. W., Saffman, P. G., and Yuen, H. C., "Calculation of Laminar Viscous Flow Over a Moving Wavy Surface," *Journal of Fluid Mechanics*, Vol. 124, 1982, pp. 347-362.

[12] Lin, J. C., Walsh, M. J., Watson, R. D., and Balasubramanian, R., "Turbulent Drag Characteristics of Small Amplitude Rigid Surface Waves," AIAA Paper 83-0228, 1983.

[13] McLean, J. W., "Computation of Turbulent Flow Over a Moving Wavy Boundary," *Physics of Fluids*, Vol. 26, No. 8, 1983, pp. 2065-2073.

[14] Viviand, H., "Conservative Forms of the Gas Dynamic Equations," *La Recherche Aerospatiale*, No. 1, 1974, pp. 65-68.

[15] Morris, P. H., "A Model for Broadband Jet Noise Amplifications," AIAA Paper 80-1004, 1980.

[16] Bradshaw, P., Cebeci, T., and Whitelaw, J. H., *Engineering Calculation Methods for Turbulent Flows*, Academic Press, London, 1981.

[17] Hsu, C. T., Hsu, E. Y., and Street, R. L., "On the Structure of Turbulent Flow Over a Progressive Water Wave: Theory and Experiment in a Transformed Wave-Following Coordinate System," *Journal of Fluid Mechanics*, Vol. 105, 1981, pp. 87-117.

[18] Hsu, C. T. and Hsu, E. Y., "On the Structure of Turbulent Flow Over Progressive Water Wave: Theory and Experiment in a Transformed Wave-Following Coordinate System, Part 2," *Journal of Fluid Mechanics*, Vol. 137, 1983,. pp. 123-153.

[19] Scott, M. R. and Watts, H. A., "Computational Solution of Linear Two Point Boundary Value Problems Via Orthonormalization," *SIAM Journal of Numerical Analysis*, Vol. 14, No. 1, 1977, pp. 40-71.